MESON PRODUCTION NEAR THRESHOLD: PHYSICS IMPLICATIONS AND NEW TECHNICAL CHALLENGES*

H.O. MEYER

Department of Physics
Indiana University
Bloomington, IN, USA

(Received December 2, 1994)

Recently, the study of pion production in few-nucleon systems has advanced considerably, mainly due to experiments using internal targets in stored, cooled beams. Experimental progress has inspired theoretical insights: from measurements close to threshold we have learned that an enhancement of the axial charge caused by heavy-meson exchange significantly contributes to pion production. The study of the production of pions, as well as heavier mesons, with stored polarized beams and polarized internal targets is likely to have important consequences for our understanding of the nuclear force.

PACS numbers: 21.45.+v

1. Introduction

Driven by technical advances, in particular the possibility of experiments with internal targets in storage rings, the study of the nucleon–nucleon (NN) interaction at low and intermediate energies has recently seen a revival.

At low energies (below the pion production threshold) the NN interaction is dominated by one-pion exchange but the exchange of multiple pions or of heavier mesons is also needed to explain the data. The study of these contributions needs a theoretical framework (*e.g.*, potential models that are constructed from individual exchange diagrams [1]) as well as high-quality NN scattering data.

---

* Presented at the XXIX Zakopane School of Physics, Zakopane, Poland, September 5–14, 1994.

As we shall see in Sect. 4.4., storage ring technology will have an important impact on the study of NN elastic scattering, in particular on the measurement of polarization observables. The main pay-off from the new experimental possibilities, however, is expected to come from a study of particle production, in particular the respective threshold regions (Sect. 2). When the reaction energy is sufficient for the constituents of the nucleonic meson field to become real they can be observed directly. The price paid is an increase in complexity of the (now inelastic) NN interaction. However, *near threshold,* production reactions are severely constrained, and the ambiguities in theoretical interpretations of the data become significantly less. This offers the possibility to isolate and discuss specific physics aspects of the NN interaction (see examples discussed in Sect. 3).

In the near future, polarization observables in particle production will become more accessible and more important in tests of theoretical ideas. The role of polarization in storage-ring experiments is discussed in Sect. 4.

2. Particle production near threshold

2.1. Why is the threshold region important?

A particle-production reaction at energies just above threshold is constrained by conservation laws. The typical near-threshold features for the case of pion production in few-nucleon systems have been summarized in a recent review article [2]; for the present purpose, let me just highlight the main points.

Within the first few hundred MeV above threshold of the reaction $NN \rightarrow NN\pi$, the angular momentum L_{NN} in the final (NN) system, as well as the angular momentum ℓ_π of the pion with respect to the NN pair, are both either 0 or 1. This restriction, together with the Pauli principle, and the conservation of angular momentum, parity and isospin greatly limits the number of partial waves that can contribute to pion production. Furthermore, the energy dependence of the cross section is well described by phase space and centrifugal barrier factors, and the final-state interaction (and, if applicable, the Coulomb repulsion) between the final-state nucleons. The partial waves with the lowest L_{NN} and ℓ_π have the weakest dependence on bombarding energy. Thus, as the bombarding energy is lowered, eventually a *single* partial wave (*e.g.*, $L_{NN} = 0$, $\ell_\pi = 0$, in short, "Ss") will remain and thus dominate the reaction.

Near threshold most of the center-of-mass kinetic energy is converted into mass, resulting in a large momentum transfer. In addition, if the quantum numbers of the exit channel are given, the angular momentum in the entrance channel is also fixed to some (low) value. Thus, the dynamical con-

straints of particle production near threshold are such that the short-range aspects of the system are emphasized.

2.2. Benefits of new technology in particle production

During the past few years, storage rings have become a new tool in nuclear physics [3]. These rings are equipped with means for phase space cooling. Cooling counteracts the growth of the phase volume of a stored beam that passes through an internal target. Stochastic cooling [4] as well as electron cooling [5] have been applied. With internal targets and intermediate energy beams electron cooling is the method of choice because of its high cooling rate. Electron cooling has been demonstrated at the Indiana Cooler [6] for protons of up to 425 MeV.

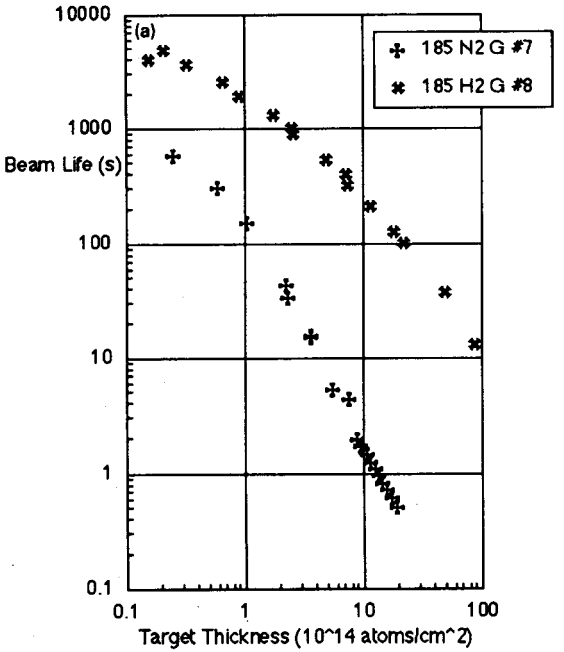

Fig. 1. Lifetimes for hydrogen and nitrogen targets for a range of target thicknesses, measured with a 185 MeV proton beam at the Indiana Cooler (from Ref. [7]).

The limited cooling force dictates a maximum target thickness which, for hydrogen, ranges from 10^{13} to 10^{16} atoms/cm^2. For thicker targets the lifetime of the stored beam becomes impractically short [7], as is illustrated in Fig. 1. Thin targets can be realized, for instance, by crossing the stored beam with a gas jet emerging from a nozzle. The stored beam is accumulated to several 100 μA, thus, even with these relatively thin targets, the resulting

luminosities are comparable to the luminosity in conventional experiments with a one-pass beam on an external target. Cooled beams typically have small emittance and a small energy spread. The beam energy is well known because it is locked to the frequency of the electric RF field that is used to bunch the stored beam. These features are especially important for measurements near threshold because of the rapid variation of the cross section with bombarding energy.

In a typical pion production measurement only the baryons in the exit channel are observed; the parameters of the pion are then reconstructed from kinematics. As an example, Fig. 2 shows the mass distribution of the unobserved third particle in $pp \rightarrow pp(m_3)$ which is deduced from the observed two outgoing protons. Close to threshold, the baryons emerge in a narrow forward cone. Thus, a detector of modest size in the forward direction is sufficient to cover all of the available phase space. The fact that the target is pure, thin, and windowless is crucial in near-threshold particle production in few-nucleon reactions. Not only does it allow the observed baryons to exit with minimal distortion, but it also avoids admixtures of heavier target nuclei for which the production threshold is much lower.

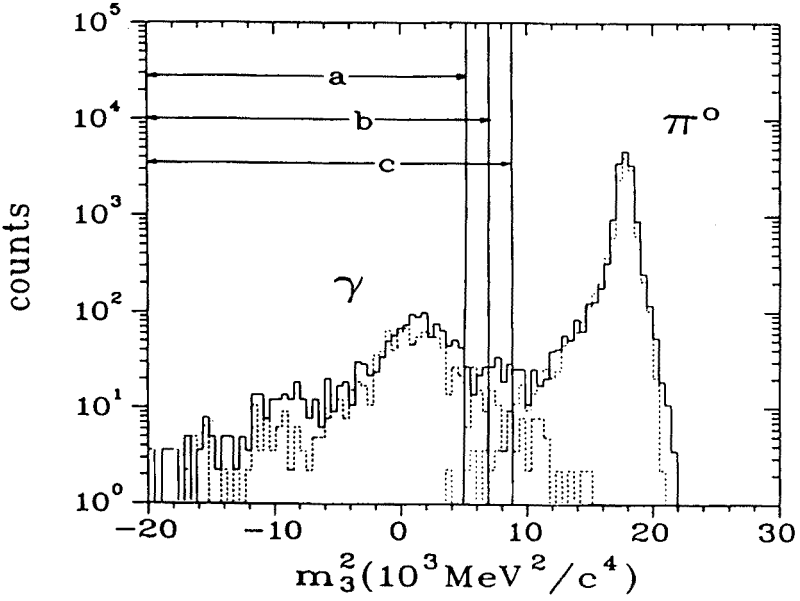

Fig. 2. Square of the mass m_3 of the particle produced in $pp \rightarrow pp(m_3)$, reconstructed from the two observed protons. The bombarding energy was 294 MeV. Peaks are seen for the two reactions $pp \rightarrow pp\pi^0$ and $pp \rightarrow pp\gamma$. The dashed line shows a Monte-Carlo simulation of the two distributions. The figure is from Ref. [38]; the cutoffs a–c were used there in separating the two processes from each other.

2.3. Pion production with the Indiana Cooler

At the Indiana Cooler, a number of pion production measurements have been carried out so far. The very first nuclear physics experiment with the new machine was, in fact, a measurement of the $pp \to pp\pi^0$ total cross section [8] near threshold (279.7 MeV). After an initial phase of rapid improvement of the machine performance, this experiment was repeated with the aim to study a possible coupling between pion production channels by searching for structure in the $pp \to pp\pi^0$ cross section near the thresholds for $pp \to d\pi^+$ and $pp \to pn\pi^+$ (287.5 MeV and 292.3 MeV, respectively). The measured cross sections are shown in Fig. 3 as a function of the customary energy parameter η (this parameter is defined as the largest possible pion center-of-mass momentum divided by the pion rest mass; at threshold $\eta = 0$ in any channel). No structure was found at the thresholds of other channels [9], but the new data, unprecedented in accuracy and closeness to threshold, led to an interesting theoretical development (see Sect. 3.1).

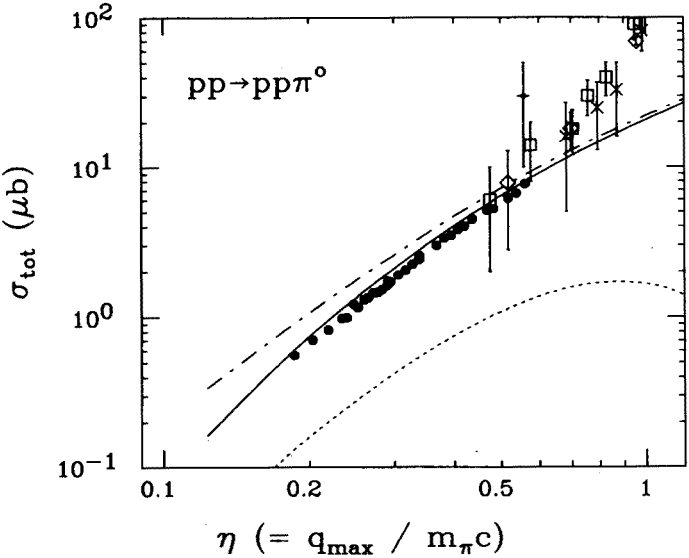

Fig. 3. Total cross section for $pp \to pp\pi^0$ as a function of η, the maximum pion momentum in the center-of-mass frame in units of m_π. The IUCF data are shown as solid dots; open symbols refer to previous work (for a list of references see Ref. [19]). A calculation with heavy-meson exchange and the Coulomb interaction is shown as a solid line. Also shown is the same without the Coulomb interaction (dash-dot line), and without heavy-meson exchange (dotted line).

The reaction $pp \to pn\pi^+$ was studied by a group from Pittsburgh University at the Cooler [10]. The first 30 MeV above threshold were covered.

Protons and neutrons were detected in coincidence. Crude magnetic separation of the reaction protons from the beam protons was made possible by a 6° bend of the Cooler orbit just downstream of the hydrogen jet target. Total cross sections as well as angular distributions were measured. The total cross section results are shown in Fig. 4.

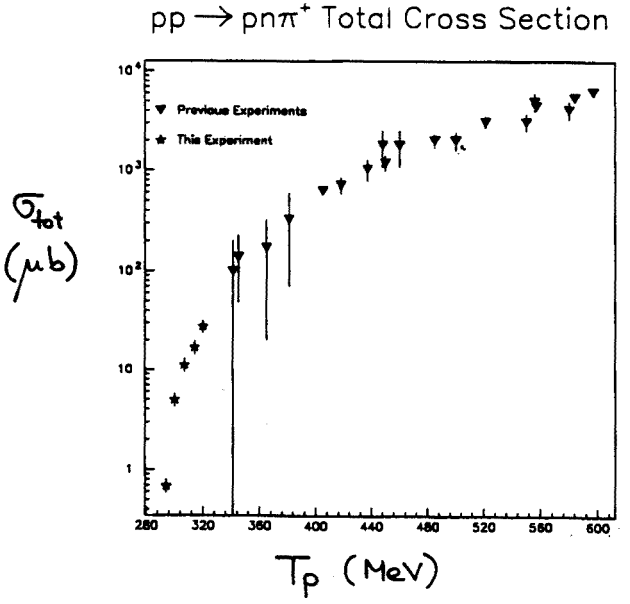

Fig. 4. Total cross section for $pp \to pn\pi^+$. Data from a recent IUCF experiment (★) are shown together with the previously available information on this reaction (▼). The figure is from Ref. [10].

Using the same technique and detector system as for the $pp \to pp\pi^0$ measurement, the total cross section for $pd \to pd\pi^0$ was studied in collaboration with a group from Hamburg [11]. The results are shown in Fig. 5 as a function of the customary energy parameter η. The total cross section is described well in terms of a quasi-free production model and the $p + d$ final-state interaction [12], using as input the "elementary" $pn \to d\pi^0$ cross section [13] which is also shown in Fig. 5. The effect of the "medium" (in this case, the presence of one spectator proton) is drastic, but it arises from conservation laws and the availability of the necessary Fermi momentum of nucleons in the target. There is no indication so far that the production vertex itself is sensitive to the presence of the extra nucleon.

In the above three cases, only the baryons in the exit channel were observed; the parameters of the pion were then reconstructed from kinematics. Observing outgoing particles in coincidence provides a clean signal

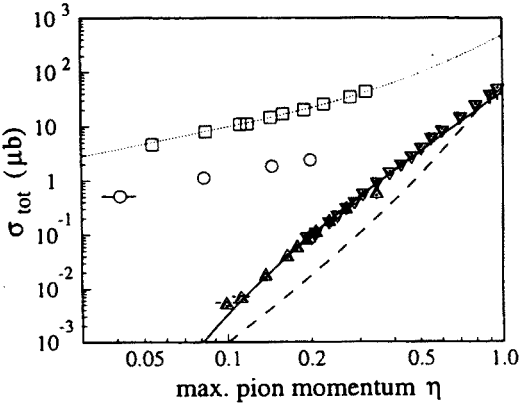

Fig. 5. Total cross sections versus η for the reactions $pd \to pd\pi^0$ (Ref. [11], triangles), $np \to d\pi^0$ (Ref. [13], squares), and $pd \to {}^3\mathrm{He}\pi^0$ (Ref. [39], circles). The dashed and dotted lines are the result of a calculation based on quasi-free production [12]. The figure is from Ref. [11].

for the reaction and is one of the reasons why data very close to threshold could be obtained. Departing from these rules, only the produced pions by themselves were detected in a measurement of $pp \to d\pi^+$ carried out in collaboration with a group from North-Western University [14]. The experiment used a polarized beam and led to cross section and analyzing power angular distributions in the range of $0.03 < \eta < 0.2$. The experiment is currently being analyzed. The results are expected to constrain the partial-wave decomposition of the channel $NN \to d\pi$ with a two-body final state.

3. Physics implications of pion production near threshold

3.1. Axial charge enhancement in $pp \to pp\pi^0$

The measurement of the total cross section of $pp \to pp\pi^0$ near threshold provides an very stringent test of pion production models because *(i)* only a single partial wave ($^3\mathrm{P}_0 \to {}^1\mathrm{S}_0 + s$-wave π^0) contributes, *(ii)* distortion due to the interaction between the nucleons is well described by an NN potential model [1], and *(iii)* production via rescattering or an intermediate $N\Delta$ state (mechanisms that are large in other $NN \to NN\pi$ channels) is suppressed as a consequence of the quantum numbers of this reaction.

Thus, there was little theoretical uncertainty when calculations [15–17] using the single-nucleon axial-charge operator (diagram (a) in Fig. 6), fell short of the measured cross section [9] by about a factor of five (an example of such a calculation is shown as dashed line in Fig. 3). At this stage it was clear that an important piece of physics must be missing in the description of this elementary process.

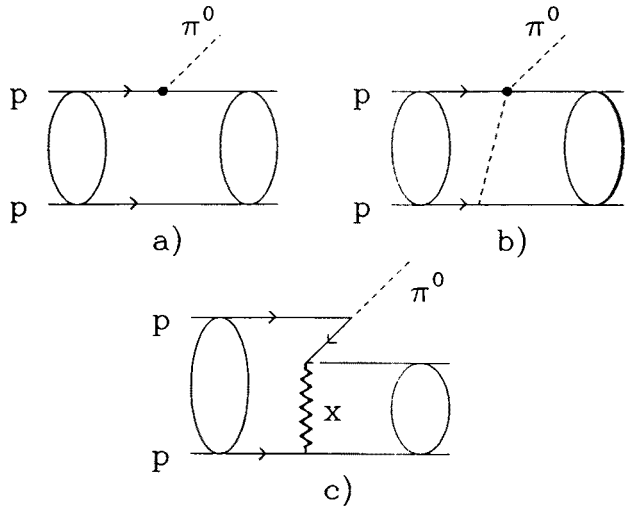

Fig. 6. Contributions to the reaction $pp \rightarrow pp\pi^0$. Shown are (a) the one-body term, (b) the two-body term that arises from pion rescattering, and (c) the two-body term that arises from the exchange of heavy mesons (x) (from Ref. [19]).

A possible explanation of this discrepancy was offered by Lee and Riska [18] who suggested that the axial charge in nuclear systems (which is responsible for s-wave pion production) is enhanced over the single-nucleon contributions. This enhancement is attributed to the exchange of heavy mesons (HME) and subsequent pion production from a nucleon-antinucleon pair, according to diagram (c) of Fig. 6. Although this (relativistic) process is a small contribution, it becomes significant for $pp \rightarrow pp\pi^0$ for which other, normally large, production mechanisms are suppressed.

In a quantitative follow-up on this idea [19], the contributions from diagram (c) in Fig. 6 were evaluated in a way that is consistent with the meson-exchange parameters of the distorting Bonn potential [1]. It was found that the main contributions to diagram (c) come from the exchange of σ and ω mesons. The two amplitudes together were found to be even larger than the one-body amplitude. Including this meson-exchange mechanism yields a quantitative description of the data (solid line in Fig. 3). Theoretical uncertainties arise from the πNN coupling constant (0.075 ± 0.003), and from

a possible non-zero rescattering term [19]. The dot-dash curve demonstrates the effect of neglecting the Coulomb interaction. The calculation also explains the energy dependence which is found to be completely determined by phase space and the low-energy behavior of the NN interaction.

The success of the HME diagram in explaining quantitatively the missing strength in the $({}^3P_0 \to {}^1S_0, \ell_\pi = 0)$ amplitude is remarkable. It is clear that $pp \to pp\pi^0$ offers an experimental window on the heavy-meson field of the nucleon and on the axial charge and current in systems of nucleons. However, how quantitative such information is, depends on the importance of other, competing production mechanisms. These involve rescattering (diagram (b) in Fig. 6) and diagrams containing Δ isobars. The contributions from rescattering have been found to be very small [17, 19] due to the smallness of the iso-scalar πN amplitudes. But for this estimate a simple, on-shell model was used for the πN interaction and the question remains whether off-shell effects are important. A similar caveat applies to a study of the role of Δ isobars [17]. More theoretical effort is clearly needed.

3.2. Role of heavy meson exchange in $NN \to (NN)\pi$

There is mounting evidence that the HME mechanism for pion production plays a significant role as well in reactions other than $pp \to pp\pi^0$. For instance, the total cross section for $NN \to d\pi$ was recently calculated [20] using a simple, distorted-wave impulse approximation. The calculation includes the one-body term, pion rescattering (calculated to lowest order), and the σ and ω meson contributions to HME. In contrast to $pp \to pp\pi^0$, the rescattering contribution to $NN \to d\pi$ is found to be large. The HME contribution is significant (about a factor of two in the cross section). When it is included in the calculation, excellent agreement results with the recently measured near-threshold cross section for $pn \to d\pi^0$ [13]. This finding is important because it tests spin and isospin matrix elements that are different from those with a pp pair in the final state. However, there are open questions. In particular, production via a Δ isobar could also be significant [21].

Following up on an earlier study [22], the reaction $\bar{p}d \to ppp\pi^-$ was recently measured at TRIUMF with polarized protons ranging in energy from 350 to 440 MeV. In the analysis of the data only events were accepted that contained a pp pair with little relative kinetic energy in the exit channel. Thus, assuming that the proton in the target acts as a spectator, information on the quasi-two-body final state reaction $\bar{p}n \to (pp)_S\pi^-$ was obtained. Angular distributions of the cross section and the analyzing power were deduced and a partial wave analysis was carried out. It was found that a large contribution arises from the $({}^3P_0 \to {}^1S_0, \ell_\pi = 0)$ amplitude (*i.e.*, the same amplitude that is responsible for $pp \to pp\pi^0$). This is in contrast with

conventional models that predict this amplitude to be very small. Inclusion of HME [23] in the calculation yields a $({}^3P_0 \rightarrow {}^1S_0, \ell_\pi = 0)$ amplitude that is in agreement with the phenomenologically determined value [24]. The theoretical interpretation of this reaction is complicated by the fact that the target neutron is originally bound in a deuteron. Whether this is correctly taken into account in the model can be tested by comparing the results of this experiment to the absorption of a π^- by a pp pair in ^{3}He, a process that differs only with respect to the "environmental" nuclear physics. At present, there are still difficulties with such a comparison [23].

4. Role of polarization observables in pion production

4.1. Theoretical motivation

As the bombarding energy increases, higher partial waves become important, but for energies for which $\eta < 1$, still only a *few* partial waves contribute. Polarization observables are sensitive to the interference between various combinations of partial wave amplitudes.

For pion-production with a two-body final state ($NN \rightarrow d\pi$) a substantial body of data is available, including data on $\pi^+ d \rightarrow pp$ which is related by detailed balance (for a review see, *e.g.*, [25]), and a partial-wave analysis can be carried out [26]. It is apparent that polarization observables are needed to constrain the parameters in such analyses.

Without a framework, such as a partial-wave decomposition, it is more difficult to relate the observables to the physics of the reaction. In special cases, however, it is still possible to isolate single partial waves. For instance, when both, polarized beam and a polarized target is available, the spin-dependent total cross sections $\Delta\sigma_L$ and $\Delta\sigma_T$ can be measured. These are defined as the difference between the cross section with the nucleon spins antiparallel minus that with the spins parallel, with both spins either along the beam axis (L), or transverse (T). Such data, in conjunction with the unpolarized total cross section σ_{tot}, provide direct information on the magnitude of the lowest three individual partial waves in $pp \rightarrow pp\pi^0$ [2]. Such a measurement which is now technically within reach and which is in preparation at the Indiana Cooler will make it possible to separate the $(L_{NN}\ell_\pi)$ Ps and Pp contributions to the $pp \rightarrow pp\pi^0$ process between 300 MeV and 400 MeV bombarding energy. This experiment is sensitive to a possible enhancement of the axial current in a Gamow–Teller transition. It is noteworthy that such information has a bearing on the solar neutrino problem [19].

4.2. Polarized beam in storage rings

The usual injection methods apply for beam delivered from a polarized ion source. Stripping injection needs incident H^- ions. At IUCF, polarized protons are injected and accumulated using phase space manipulation in conjunction with electron cooling. Typical fill rates are about 50 μA/min. The beam, polarization is typically 70%. When the intensity has reached several hundred μA the stored beam is accelerated to the desired energy, then the experiment starts to acquire data.

For a ring with only vertical magnetic fields, the stored polarization is quite stable, except at discrete beam energies for which the precession frequency of the magnetic moment of a stored particle is an integer multiple of the frequency of some non-vertical perturbing field. Such fields can arise from non-ideal optics (causing "imperfection resonances") or from the transverse field of the focussing quadrupoles (causing "intrinsic resonances"). The precession frequency $f_{\mathrm{prec}} = G\gamma f_{\mathrm{orb}}$ of the magnetic moment of a proton ($G = 1.793$) around the bend field direction (vertical), is synchronous, in the first case with the orbit frequency f_{orb}, and in the second case with the vertical betatron frequency $\nu_z f_{\mathrm{orb}}$. For a comprehensive treatment of polarization in a ring, see Refs [27, 28].

If care is taken to avoid the critical energies and machine tunes, the beam polarization is remarkably stable. From the combined data from several IUCF experiments that were carried out with polarized protons there now seems to be some indication of a small, but finite depolarization rate, $(-1/P)(dP/dt)$, in the presence of an internal target. The time over which the polarization could be observed ranged between 400 s and 700 s. A possible explanation of beam depolarization was found in coupling to the nearest depolarizing resonances due to scattering from the target. This model predicts that the depolarization rate is proportional to the beam lifetime. This prediction together with the measurements is shown in Fig. 7.

Of importance to the systematics of polarization measurements with a storage ring is the possibility to reverse the polarization of the stored beam. This can be achieved by an oscillating longitudinal magnetic field with a frequency f_{osc} close to the precession frequency, f_{prec}, of the stored particles. When f_{osc} is varied across f_{prec}, the polarization flips. Development of this tool is still in progress; so far, it has been demonstrated that more than 94% of the original polarization survives the flip [29].

The presence of static, non-vertical fields does not affect the magnitude of the beam polarization. However, it does change the direction in which the polarization of a stored beam is stable. This direction depends on the location along the trajectory, and makes possible experiments with beams polarized in directions other than vertical. This has been demonstrated in the Indiana Cooler in a study of the effect of a longitudinal solenoid field on

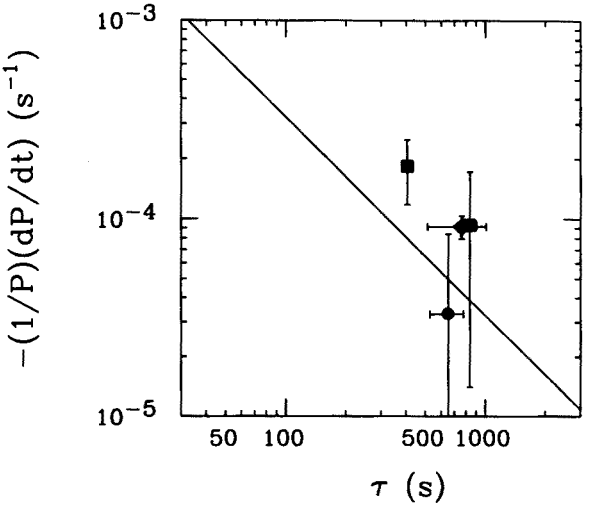

Fig. 7. Depolarization rate of a proton beam in the presence of a H_2 target as a function of the beam lifetime τ. The data indicated by squares are obtained at 200 MeV [40], the diamond indicates a measurement at 300 MeV [14]. The solid line is the expectation from a model that evaluates the coupling to the nearest intrinsic resonance that results from scattering in the target [41].

the polarization of stored protons [30]. Experiments in which longitudinal solenoid fields will be used to establish sideways and longitudinal beam polarization at the target location are planned for the near future at IUCF.

4.3. Polarized, internal targets

Using a source of polarized atoms, polarized internal targets of a useful thickness are conceivable. To overcome the severe limits in the production rate of polarized atoms, the use a "storage cell" has been proposed [31]. The purpose of such a cell is to increase the dwell time of target atoms near the beam, and thus the target thickness by a factor of several hundred compared to using the atomic beam as a jet target. Since the atomic beam is free of impurities and the cell is open at both ends, the stored beam interacts only with the target nuclei of interest.

The implications of the presence of a narrow storage cell with respect to the performance of the storage ring and a possible experiment have been studied at IUCF [32]. Recently, a polarized ^{3}He target, produced by optical pumping, has been used at IUCF [33]; its polarization ($P \sim 0.4$) was determined via $p + {}^3$He elastic scattering. A $\overline{H}$ target, produced with an atomic beam source was previously operated at the TSR ring of the Max-Planck Institute in Heidelberg [34].

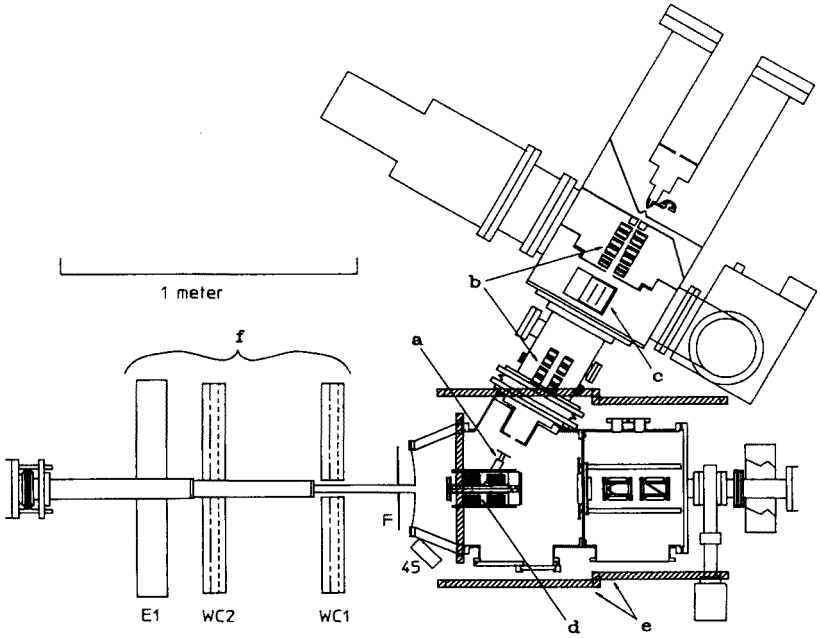

Fig. 8. Top view of the polarized target setup in the A-region of the Indiana Cooler. Shown are the atomic beam source with sextupoles (b) and RF transition (c), the target cell with feed tube (a), the detectors (F, 45 d, f, see also Fig. 10), and the guide field coils (e). The stored beam travels from right to left.

Currently, a polarized hydrogen target [35] is installed in the Indiana Cooler, and extensive experience with such a device is being gained. A top view of the layout is shown in Fig. 8. The atomic beam source uses permanent-magnet sextupole separators (b) in conjunction with RF transitions (c) to filter out $\overline{\mathrm{H}}$ atoms in a single spin state. The source is described in detail in Ref. [36]. The atomic beam is aimed at the feed tube (a) of the 25 cm long target cell. The open aperture of the cell, through which the proton beam of the Cooler passes, is an 8 mm×8 mm square [35]. The target thickness is determined from *pp* elastic scattering, using the known pp cross section, beam current and detector solid angle. An example of such a measurement over the duration of an experimental run is shown in Fig. 9. The measured target thickness of $3.2 \times 10^{13} \overline{\mathrm{H}}/\mathrm{cm}^2$, is in agreement with the value of 3.5×10^{16} atoms/s, predicted [35] from the measured atomic-beam intensity and the gas conductance of the cell (these figures are for the case where the source produces a single spin state).

An extensive study has been conducted to find a material for the interior surface of the cell which has good vacuum characteristics and minimizes the depolarization of atoms when they collide with the cell walls [37]. The

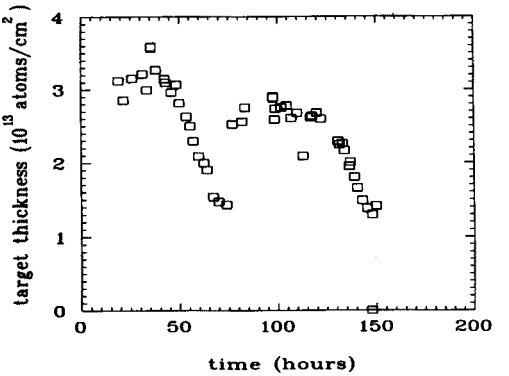

Fig. 9. Polarized-target thickness over the duration of an experimental run. The periodic decrease of the thickness is caused by clogging of the nozzle (usually at liquid nitrogen temperature) of the dissociator in the source. It can be cured by warming up the nozzle.

present IUCF target uses walls that are either thin Teflon foil or Teflon-coated aluminum. The target polarization was measured via $p + p$ elastic scattering with a stored beam of 200 MeV protons to be about 70%. From the measured polarization along the target cell an upper limit of 6×10^{-4} was deduced for the depolarization per wall collision (the average atom, found in the center of the cell has undergone about 100 wall collisions, and about twice as many when near the end of the cell). It was found that the performance of the Teflon wall does not change with prolonged running, *i.e.*, it is immune to radiation damage. This is of course also true for the atomic target itself which is renewed about every millisecond.

The direction of the target polarization is determined by a weak magnetic guide field (of the order of 10 Gauss). This field is generated by coils placed on the outside of the target chamber ((e) in Fig. 8), making it possible to polarize the target horizontally ($\pm x$), vertically ($\pm y$), and along the beam directions ($\pm z$). The direction of polarization can be changed rapidly: the measured polarization rise time after switching is less than 50 ms. The effect of the transverse guide fields on the trajectory of the stored beam is compensated by additional fields upstream and downstream of the target.

4.4. Spin correlation measurements with the Indiana Cooler

As mentioned earlier, it is planned to use he Indiana Cooler to measure spin-dependence in the total cross section for $pp \to pp\pi^0$. The development of the necessary experimental capabilities is currently in progress. As part of this process, a measurement of spin correlation coefficients in pp elastic scattering will be carried out. Thus, experimental information will be gained

about the NN system below threshold in an energy range where only a few previous measurements of spin correlation coefficients exist.

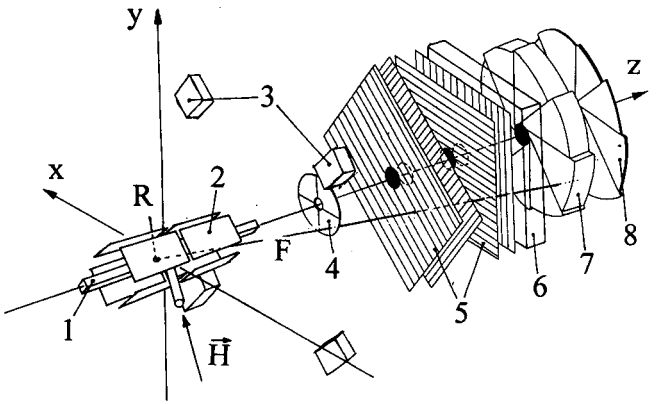

Fig. 10. Detector setup to measure spin correlation coefficients in pp elastic scattering. The stored beam travels along the z axis. Polarized atoms ($\vec{H}$) enter the storage cell (1). Forward protons (F) are measured by a stack of detectors consisting of a thin scintillator (4), four wire chamber planes (5), an aluminum absorber (6) and two segmented scintillator planes (7,8). Recoil protons (R) are measured in coincidence by eight position-sensitive microstrip detectors (2). Four small scintillators (3) detect scattering events at 90° in the c.m. system.

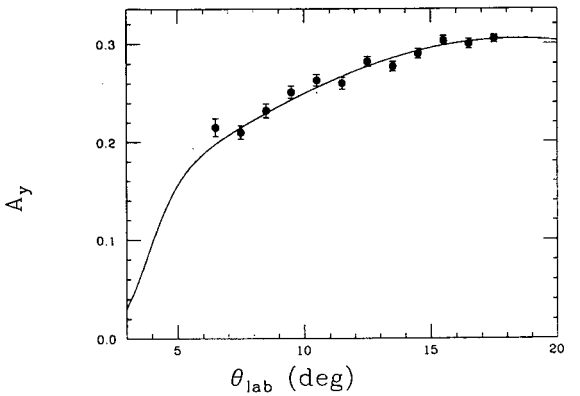

Fig. 11. Analyzing power Ay for pp elastic scattering at 200 MeV, obtained with a polarized beam in the Indiana Cooler [40]. The solid curve is the prediction by the C200 solution from the 1994 version of SAID [42].

At present, the first phase of this program is nearing completion. In this phase, the spin correlation coefficients A_{xx}, A_{yy} and A_{zz} for pp scattering

have been measured at 200 MeV. The detector system is shown in Fig. 10. To suppress unwanted background on the 1% level, the forward scattered proton (F) is detected in coincidence with the recoil proton (R). The recoil proton is detected by eight position-sensitive, silicon micro-strip detectors. This allows the reconstruction of the vertex of every event, which in turn yields valuable information on the performance of the polarized target. A preliminary measurement of the analyzing power angular distribution is shown in Fig. 11, together with a recent phase shift prediction. The angular region that is covered by this experiment overlaps the region of Coulomb-nuclear interference. Such data are stringently constraining the parameters of phase shift analyses.

Future extension of the measurement of pp elastic scattering include bombarding energies from 100 to 500 MeV, as well as the measurement of the spin correlation coefficient A_{zz} of which requires longitudinal beam polarization.

5. Summary

The study of meson production is particularly interesting near threshold, where conservation laws severely restrict the number of participating angular momentum states. This has been demonstrated in the case of pion production, where recent, accurate total cross section measurements have led to new insights about the short-range component of the NN interaction and the coupling of the meson field to the nucleon.

The measurement of high-quality data very close to threshold has been made possible to a large part by the use of a stored, electron-cooled proton beam in conjunction with an internal target. This new technology naturally lends itself to the use of polarized internal targets which are pure, windowless and free of radiation damage. Thus, measurements of polarization observables, in particular spin correlation coefficients and spin-dependent total cross sections, are possible with a storage ring. The first such measurements for pp elastic scattering are presently carried out at Indiana. The new data are expected to provide more stringent constraints of phase shift analyses of pp scattering, as well as information about individual partial waves in pion production near threshold.

One can expect that the experience gained with the new technology and the theoretical ideas that are caused by measurements near the pion threshold will provide the basis of studies of the production of heavier mesons with storage rings at higher energies.

REFERENCES

[1] R. Machleidt, *Adv. Nucl. Phys.* **19**, 189 (1989).

[2] H.O. Meyer, *Phys. Scr.* **48**, 54 (1993).

[3] R.E. Pollock, *Ann. Rev. Nucl. Sci.* **41**, 357 (1991).

[4] D. Möhl, G. Petrucci, L. Thorndahl, S. van der Meer, *Phys. Rep.* **58**, 73 (1980).

[5] H. Poth, *Phys. Rep.* **196**, 135 (1990).

[6] R.E. Pollock, Proc. IEEE Particle Accelerator Conf., Chicago 1989, eds. F. Bennett and J. Kopta, IEEE Conf., 1989, p.17.

[7] R.E. Pollock, V. Derenchuk, X. Pei, T. Sloan, F. Sperisen, H.O. Meyer, B. v. Przewoski, T. Rinckel, P. Pancella, M.A. Ross, W.K. Pitts, *Nucl. Instr. Meth.* **A330**, 380 (1993).

[8] H.O. Meyer *et al.*, *Phys. Rev. Lett.* **65**, 2846 (1990).

[9] H.O. Meyer, C. Horowitz, H. Nann, P.V. Pancella, S.F. Pate, R.E. Pollock, B. v. Przewoski, T. Rinkel, M.A. Ross, F. Sperisen, *Nucl. Phys.* **A539**, 633 (1992).

[10] W.W. Daehnik, Proc. 5-th Int. Symp. on Meson-Nucleon Physics, Boulder , Colorado, Sept 6-10, 1993, πN Newsletter no.**8**, eds. G. Hoeler, W. Kluge and B.M. Nefkens, 1993, p.105.

[11] H. Rohdjess, W. Scobel, H.O. Meyer, P.V. Pancella, S.F. Pate, M.A. Pickar, R.E. Pollock, B. v.Przewoski, T. Rinckel, P.P. Singh, F. Sperisen, L. Sprute, *Phys. Rev. Lett.* **70**, 2864 (1993).

[12] H.O. Meyer, J.A. Niskanen, *Phys. Rev.* **C47**, 2474 (1993).

[13] D.A. Hutcheon, E. Korkmaz, G.A. Moss, R. Abegg, N.E. Davison, G.W.R. Edwards, L.G. Greeniaus, D. Mack, C.A. Miler, W.C. Ohlsen, I.J. van Heerden, Y.E. Yanlin, *Nucl. Phys.* **A535**, 618 (1991).

[14] Differential Cross Section and Analyzing Power of $p(\vec{p}, \pi^+)d$ near Threshold, P. Heimberg *et al.*, IUCF, Scientific and Technical Report 1992–93, eds E. Stephenson and C. Olmer, IUCF 1994.

[15] D.S. Koltun, A. Reitan, *Phys. Rev.* **141**, 1413 (1966).

[16] G.A. Miller, P.U. Sauer, *Phys. Rev.* **C44**, R1725 (1991).

[17] J.A. Niskanen, *Phys. Lett.* **B289**, 227 (1992).

[18] T.S. Lee, D.O. Riska, *Phys. Rev. Lett.* **70**, 2237 (1993).

[19] C.J. Horowitz, H.O. Meyer, D.K. Griegel, *Phys. Rev.* **C49**, 1337 (1994).

[20] C.J. Horowitz, *Phys. Rev.* **C48**, 2920 (1993).

[21] J.A. Niskanen, Helsinki, private communication.

[22] C. Ponting *et al.*, *Phys. Rev. Lett.* **63**, 1792 (1989).

[23] J.A. Niskanen, *Phys. Rev.* **C49**, 1285 (1994).

[24] P. Walden, TRIUMF, private communication.

[25] H. Garcilazo, T. Mizutani, πNN Systems, World Scientific, Singapore, 1990.

[26] D.V. Bugg, *J. Phys. G: Nucl.Phys.* **10**, 47 (1984).

[27] S.Y. Lee, *Phys. Rev.* **E47**, 3631 (1993).

[28] R.E. Pollock, Proc. Workshop on Physics with Polarized Beams on Polarized Targets, (McCormick's Creek, October 1989), eds J. Sowinski and S.E. Vigdor, World Scientific, 1990, p.372.

[29] B. v.Przewoski, Indiana Universtity Cyclotron Facility, private communication.
[30] A.D. Krisch, S.R. Mane, R.S. Raymond, T. Roser, J.A. Stewart, K.M. Terwilliger, B. Vuaridel, J.E. Goodwin, H.O. Meyer, M.G. Minty, P.V. Pancella, R.E. Pollock, T. Rinckel, M.A. Ross, F. Sperisen, E.J. Stephenson, E.D. Courant, S.Y. Lee, L. G. Ratner, *Phys. Rev. Lett.* **63**, 1137 (1989).
[31] W. Haeberli, Proc. Workshop on Nuclear Physics with Stored, Cooled Beams, McCormick Creek State Park 1984, ed. P. Schwandt and H.O. Meyer, AIP Conf. Proc. **128**, 1985, p.251.
[32] Test of a Windowless Storage Cell Target in a Proton Storage Ring, M.A. Ross, W.K. Pitts, W. Haeberli, H.O. Meyer, S.F. Pate, R.E. Pollock, B. v. Przewoski, T. Rinckel, J. Sowinski, F. Sperisen, P. Pancella, *Nucl. Instr. Meth.* **A326**, 424 (1993).
[33] K. Lee *et al.*, *Phys. Rev. Lett.* **70**, 738 (1993).
[34] F. Rathmann, C. Montag, D. Fick, J. Tonhaeuser, W. Brueckner. H.-G. Gaul, M. Grieser, B. Povh, M. Rall, E. Steffens, F. Stock, K. Zapfe, B. Braun, G. Graw, W. Haeberli, *Phys. Rev. Lett.* **71**, 1379 (1993).
[35] M.A. Ross, A.D. Roberts, T. Wise, W. Haeberli, W.A. Dezarn, J. Doskow, H.O. Meyer, R.E. Pollock, B. v. Przewoski, T. Rinckel, J. Sowinski, F. Sperisen, P. Pancella, *Nucl. Instr. Meth.* **A344**, 307 (1994).
[36] T. Wise, A.D. Roberts, W. Haeberli, *Nucl. Instr. Meth.* **A336**, 410 (1993).
[37] S. Price, W.Haeberli, *Nucl. Instr. Meth.*, to be published.
[38] B. v.Przewoski, H.O. Meyer, H. Nann, P.V. Pancella, S.F. Pate, R.E. Pollock, T. Rinckel, M.A. Ross, F. Sperisen, *Phys. Rev.* **C45**, 2001 (1992).
[39] M.A. Pickar, A.D. Bacher, H.O. Meyer, R.E. Pollock, G.T. Emery, *Phys. Rev.* **C46**, 397 (1992).
[40] T. Wise *et al.*, Spin-Polarized Internal Gas Target for Hydrogen and Deuterium at the IUCF Cooler Ring; W.A. Dezarn *et al.*, Spin Correlation Coefficients in pp Elastic scattering at 200 MeV; T. Rinckel *et al.*, Technique for making Spin Correlation Measurements at the IUCF Cooler, contributions to 8-th Int. Symp. on Polarization Phenomena in Nuclear Physics, Sept 15-22, 1994, Bloomington, IN, USA.
[41] H.O. Meyer and B. v.Przewoski, Beam Depolarization with an Internal Target, contribution to 8-th Int. Symp. on Polarization Phenomena in Nuclear Physics, Sept 15-22, 1994, Bloomington, IN, USA.
[42] R.A. Arndt *et al.*, *Phys. Rev.* **D45**, 3995 (1992).